EDGE ARTICLE

ROYAL SOCIETY OF CHEMISTRY

Check for updates

All publication charges for this article have been paid for by the Royal Society of Chemistry

Catalytic asymmetric P(III)-additions to salicylaldehydes enable divergent stereoselective dearomatizations of phenols

Aidan J. Clarkson, [iD] † Kimberly A. Alley, [iD] † Bryn K. Werley, [iD] Jacob G. Robins, [iD] Shubin Liu [iD] and Jeffrey S. Johnson [iD] *

Oxidative dearomatizations are useful tools in complex molecule synthesis and the development of enantioselective variants offers substantial opportunities for the field. In this article, we describe a platform for a formal enantioselective dearomatization that employs chiral nonracemic α-hydroxyphosphonates derived from salicylaldehydes to direct diastereoselective functionalization of the phenolic core. As a requisite first step, we developed a new bis(oxazoline)Cu(II)-catalyzed hydrophosphonylation (Pudovik reaction) of salicylaldehydes, allowing access to enantioenriched material in one step. The derived α-hydroxyphosphonates participated in complementary stereoselective dearomatization sequences. A tandem phosphono-Adler–Becker oxidation/[4 + 2]-cycloaddition furnished bicyclo[2.2.2]-octanes bearing phosphonoepoxyketone functionalities in excellent regio- and diastereoselectivity for both steps. Alternatively, oxidation with phenyliodine(III) diacetate (PIDA) provided access to either 2,5- or 2,4-cyclohexadienones, with the latter reacting in a complementary [4 + 2]-cycloaddition. Experimental and computational studies of the two paths reveal distinct modes of stereochemical relay from the α-hydroxyphosphonate adducts to the derived dearomatized Diels−Alder products. The removable α-hydroxyphosphonate and phosphonoepoxide functionalities enable downstream synthetic modifications to the stereochemically defined cycloadducts.

Introduction

Enantioselective phenol dearomatization is a desirable tool in small molecule synthesis, providing access to the latent functionality within the nucleus of readily available hydroxyarene feedstocks.[1] This enabling paradigm reveals useful reactive nonaromatic building blocks (Scheme 1A), but it can carry limitations associated with electronic constraints of the substrate and catalyst (i), inherent characteristics of the reaction mechanism (ii),[2] and the challenges associated with overcoming aromatic stabilization energy.[3] Current methods for enantioselective phenol dearomatization[1,4] invoke the use of reagents such as hypervalent iodine,[5–8] enzymes,[9] transition metals,[10,11] or chiral phase transfer catalysts,[12] with varying degrees of success and efficiency. Among these examples, naphthol dearomatizations are comparatively more common, although highly enantioselective catalytic phenol spirolactonizations[6,7] serve to demonstrate the functional group tolerance of chiral hypervalent iodine oxidations and the promise of the approach. Advances in enantioselective dearomative fluorination reactions of both naphthols and phenols
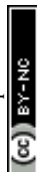
reveal the continual progression of this field.[13–15] These examples simultaneously allude to the extant challenges in developing complementary enantioselective oxidative dearomatization reactions with the same degree of selectivity and generality.

Within the scope of readily available phenols, salicylaldehydes might possess a unique opportunity for stereo-differentiating dearomatization reactions.[16] We hypothesized that heretofore unknown enantioselective aldehyde additions could be leveraged as a source of absolute stereochemical information to be relayed through a diastereoselective dearomatization/cycloaddition sequence to access value-added complex cyclohexanes (Scheme 1B). A key facet of this approach is the decoupling of the asymmetric catalysis (I → II, step 1) and dearomatization events (II → III/IV, step 2), which we anticipated would confer greater synthetic flexibility by permitting variable oxidation conditions to access distinct nonaromatic products (III and IV). Strategically, the source of chirality would ideally serve as a versatile functional handle for downstream transformations and thwart unwanted reactivity at the carbonyl – protecting it – until later in the sequence.
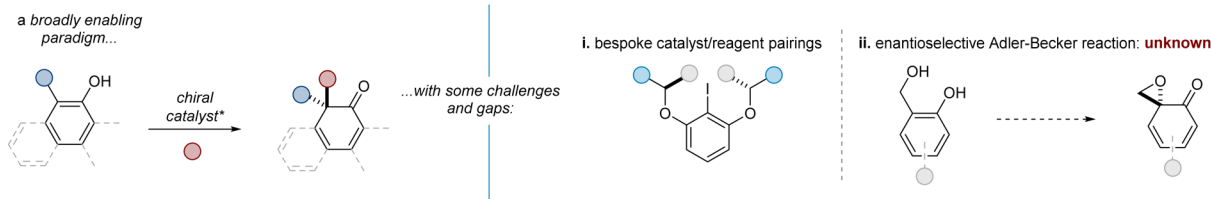
With these design criteria in mind, the use of α-hydroxyphosphonates was considered.[17–28] Their stereocontrolled synthesis is usually accomplished through the addition of a tri- or pentavalent phosphorus compound to an aldehyde (i.e., the

Department of Chemistry, University of North Carolina at Chapel Hill, Chapel Hill, North Carolina 27599-3290, USA. E-mail: jsj@unc.edu
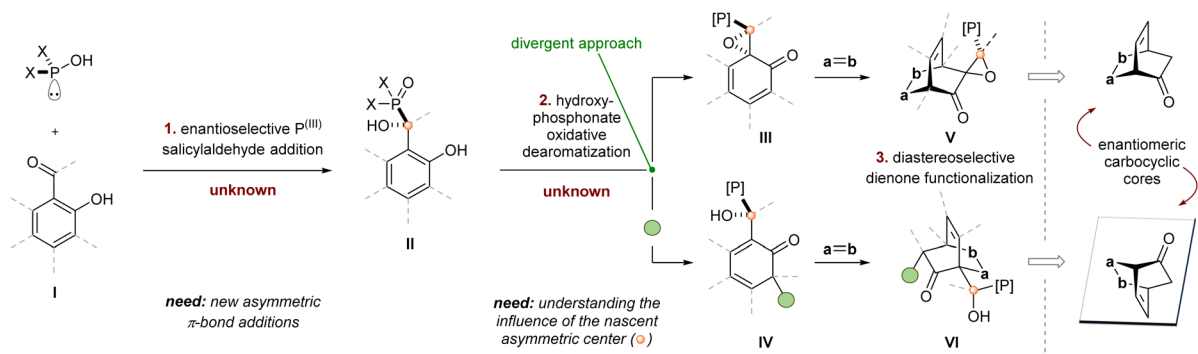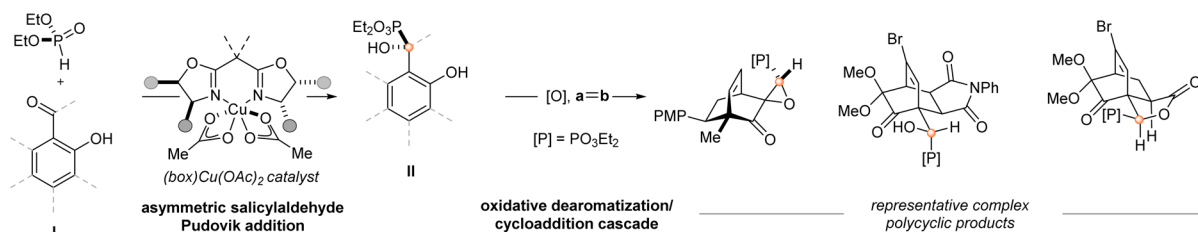
† These authors contributed equally.

Scheme 1 Proposed reaction platform for enantioselective dearomatization of salicylaldehydes.

Pudovik reaction),[29] which has been shown to be reversible under alkaline conditions.[21,25,30,31] We sought to employ chiral nonracemic α-hydroxyphosphonates (**II**) derived from salicylaldehydes (**I**) as a point of entry to value-added complex cyclohexanes (**V** and **VI**) *via* oxidative dearomatizations of salicyl alcohol derivatives. Furthermore, we hoped to expand the possible product diversity by employing either a dearomative epoxidation (Adler–Becker oxidation) or an oxidation with phenyliodine(III) diacetate (PIDA).[32,33] While the latter has been demonstrated enantioselectively,[6,7] there are no known examples of an enantioselective variant of the former.[2] This point is further emphasized by a recent report that demonstrates both the challenges and potential utility of the Adler–Becker reaction in complex molecule synthesis.[34] We envisioned that this integrated strategy might enable access to enriched dearomatization products through either oxidation pathway, relying instead on the ability of the nascent stereogenic hydroxyphosphonate to induce diastereoselectivity in the dearomatization/cycloaddition cascade. Literature precedent[13,35–39] suggested the possibility of applying related tandem oxidative dearomatization/Diels–Alder reactions to trap the resulting dienones (Scheme 1B, step 3); however, this work would have several key distinctions. First, this method would provide access to cycloadducts in enantioenriched fashion, which has not been

achieved previously using Adler–Becker oxidation chemistry. Second, we anticipated that slow or reversible diene dimerization might allow for a greater scope of employable dienophiles relative to the prior art. Lastly, the phosphonate functionality would serve as a functional handle for enhanced synthetic utility.

Several potential reactivity and stereochemical challenges emerged upon consideration this experimental plan. First, there are scant reports for the synthesis of racemic salicyl α-hydroxyphosphonates[40,41] and no extant methods for accessing enantioenriched variants, a circumstance that stands in contrast to the plethora of reported reactions for other benzaldehydes.[42–49] Enantioselective nucleophilic additions of other nucleophiles to salicylaldehydes are known,[50–55] but they are usually illustrated as single examples within a scope of benzaldehydes. One reason for this rarity may be the acidic nature of the phenolic proton, which results in deactivation of the electrophile upon deprotonation by a basic catalyst. Second, the phosphonate group's impact on the efficiency and selectivity of the oxidative dearomatization and subsequent dienone functionalization was an open question. Adler–Becker reactions in which the aryl-benzylic C–C bonds experience free rotation are rare and exhibit variable stereocontrol.[56–58] Lastly, we suspected that the presence of the phosphonate might affect the

well-established propensity of cyclohexadienones to dimerize by [4 + 2]-cycloaddition.[1,11,59–62]

Herein, we describe an integrated approach to stereoselective dearomatization reliant on the development of a new enantioselective Cu(II)-catalyzed addition of P[(III)] nucleophiles to salicylaldehydes (Scheme 1C). The derived α-hydroxyphosphonates can be processed by distinct oxidative dearomatization paths to give dienone intermediates that participate in diastereoselective cycloadditions operating under divergent stereocontrol mechanisms; consequently, Pudovik adducts are convertible to chiral building blocks with enantiomeric carbocyclic core structures and complementary peripheral functionality based on the oxidation path selected.
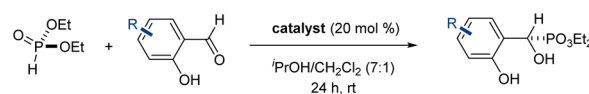
Results and discussion

Development of a copper-catalyzed hydrophosphonylation of salicylaldehydes

Our initial efforts began with investigating the asymmetric Pudovik reaction using a bis(oxazoline)Cu(II) (box) complex. Work by Evans and coworkers demonstrated that a (box)Cu(II) complex bearing mildly basic acetate ligands promotes the asymmetric nitroaldol reaction of aldehydes.[63] Based on the similar pK_a values of dialkyl phosphites and nitroalkanes,[64,65] we speculated that a similar system might successfully promote the title reaction; however, salicylaldehyde is absent from the Evans work, making a direct comparison difficult. Direct application of literature conditions from a catalytic hydrophosphonylation of aryl and styrenyl aldehydes[48] to our desired
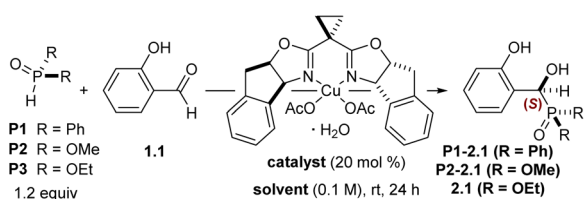
substrate (salicylaldehyde **1.1**) highlighted the unique challenges posed by salicylaldehydes, affording the desired product in 25% yield (by ^{1}H NMR spectroscopy) and 51 : 49 er. Further experiments revealed that 20 mol% of an *in situ* prepared inda(box)Cu(II) complex (Table 1) catalyzed nucleophilic addition of diphenylphosphine oxide to salicylaldehyde **1.1** in good yield but poor enantioselectivity (entry 1). Using dimethyl phosphite and switching from THF to MeOH as the solvent

Table 2 Reaction scope of the copper bis(oxazoline)-catalyzed asymmetric Pudovik reaction of salicylaldehydes

2.1 yield 85% er 90:10	**2.2** yield 45% er 95:5	**2.3** yield 68% er 92:8
2.4 yield 63% er 92:8	**2.5** yield 61% er 93:7	**2.6** yield 48% er 93:7
2.7 yield 76% er 87:13	**2.8** yield 77% er 90:10	**2.9** yield 70% er 88:12
2.10 yield 39% er 87:13	**2.11** yield 48% er 90:10 (>99:1)[a]	**2.12** yield 51% er 96:4
without phenolate chelation		
2.13 yield 49% (78%)[b] er 90:10	**2.14**[c] yield 15% er 61:39	**2.15**[d] yield 0% er n.d.
challenging substrates		
2.16 yield 0% er n.d.	**2.17**[d] yield 21% er n.d.	**2.18**[c] yield 14% er n.d.

[a] Enantiomeric ratio after recrystallization from CH_2Cl_2. [b] Reaction run on 5.0 mmol scale. [c] NMR yield. [d] EtOH, 1.2 equiv. phosphite.

Table 1 Abbreviated optimization of the catalytic asymmetric Pudovik reaction

Entry	Solvent	Phosphite	Yield[a] (%)	er[b]
1	THF	P1	72	65 : 35
2	MeOH	P2	n.d.	81 : 19
3	THF	P3	63	82 : 18
4	MeCN	P3	21	81 : 19
5	DCM	P3	10	81 : 19
6	Et₂O	P3	42	81 : 19
7	MeOH	P3	47	87 : 13
8	EtOH	P3	58	90 : 10
9[c]	EtOH	P3	95	88 : 12
10[d]	iPrOH	P3	86	88 : 12
11[d]	CH₂Cl₂/iPrOH (1 : 10)	P3	90	90 : 10
12[d]	**CH₂Cl₂/iPrOH (1 : 7)**	**P3**	**97**	**90 : 10**

[a] Yields determined by ^{1}H NMR spectroscopic analysis using phenanthrene as an internal standard. [b] Enantiomeric ratio determined by HPLC analysis. [c] Reaction performed at 0.5 M using 1.5 equiv. phosphite. [d] Reaction performed at 0.25 M using 1.5 equiv. phosphite.

produced a marked improvement in enantioselectivity (entry 2). Using diethyl phosphite, the reaction proceeded with moderate selectivity in various solvents (entries 3–6), with methanol providing the α-hydroxyphosphonate **2.1** in 47% NMR yield and 87 : 13 er (entry 7). The use of diisopropyl phosphite was also evaluated but showed decreased yield with respect to diethyl phosphite (not shown). Several other box, py(box), and inda(-box) ligands were screened (see SI for additional optimization details), but no other ligand further improved the observed enantioselectivities. A solvent screen revealed that protic solvents gave markedly higher rates of conversion and selectivities, with isopropanol and ethanol outperforming other branched and straight-chain alcohols. This trend in coordinating solvents is in agreement with other (box)Cu(II)-catalyzed aldehyde additions.[66] Lowering the reaction temperature to 0 °C reduced conversion and yield by 10% and had no impact on the enantioselectivity. Increasing the reaction temperature or extending the reaction times also did not produce a significant change to the enantioselectivity. The catalyst loading could be reduced to 5 mol% with no impact on enantioselectivity; however, increased catalyst loadings enabled full conversion of starting material while only requiring 1.5 equivalents of phosphite at 0.5 M (entry 9). Ultimately, isopropanol was used instead of ethanol due to increased conversion and consistency across all substrates. Small amounts of dichloromethane as a cosolvent were found to promote more complete conversion of starting material with negligible effect on enantioselectivity (entries 11 and 12).

The system tolerated both electron-poor and electron-rich arenes as well as various substitution patterns on the arene, providing α-hydroxyphosphonates in moderate to good yields

with enantiomeric ratios equal to or exceeding 87 : 13, with most products equal to or exceeding 90 : 10 er (Table 2). The enantiomeric ratio of α-hydroxyphosphonate **2.11** was further upgraded by recrystallization from dichloromethane, affording the desired product as a single observable enantiomer by chiral HPLC. The reactions could be scaled up to at least 5.0 mmol scale without detriment to the yield or enantioselectivity of the transformation. Arenes with substitution at the 6-position proved challenging in this system (**2.16–2.18**), likely due to steric crowding during phosphite addition.

The configuration of the new asymmetric center was established as (*S*) through an X-ray diffraction study of a derivative (*vide infra*). This stereochemical outcome constitutes a reversal in aldehyde enantiotopic facial preference relative to prior art,[63] indicating a probable change in stereocontrol mechanism. The unique nature of the salicylaldehyde electrophile emerged as the most probable source of this stereochemical reversal. As a point of departure, we formulated a simple mechanism for evaluation. Twofold X-ligand exchange in the (indabox) Cu(OAc)$_2$ complex with one equivalent each of salicylaldehyde and diethyl phosphite was proposed to liberate HOAc (2 equiv.) and create the reactive ternary complex **(indabox)Cu-A** (Fig. 1). Maximal LUMO-lowering Lewis acid activation of the carbonyl should occur in the ligand plane and optimal HOMO-raising activation of the nucleophilic phosphite should be realized in the apical site, consistent with precedent and established trends with Cu(II).[67] When the (indabox)Cu(OAc)$_2$ complex was treated with 3,5-dibromosalicylaldehyde (**1.11**, 2 equiv.), the crystalline bis(phenolate) octahedral complex (indabox) Cu(**1.11**)$_2$ was obtained through X-ligand exchange (Fig. 1). As expected, based on Jahn–Teller considerations,[63,67] the phenolate ligands lie in the ligand plane while the chelating aldehydes
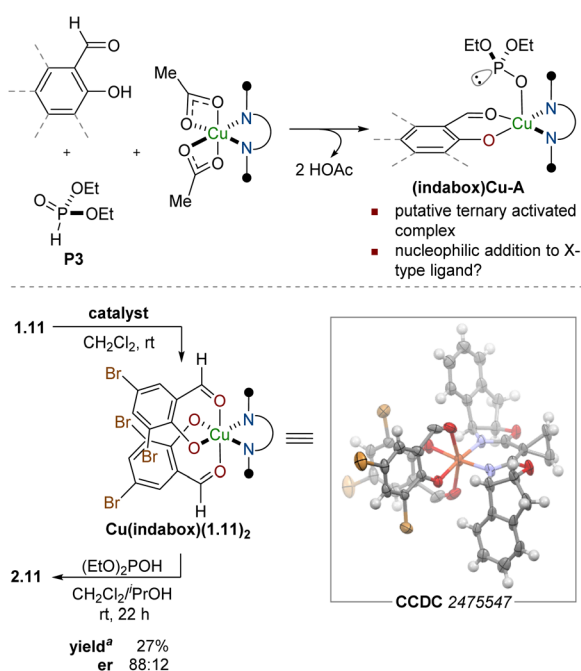

Fig. 1 Simplified mechanistic scheme and a test of ligand exchange. [a] Yield determined by ^{1}H NMR spectroscopic analysis using mesitylene as an internal standard.
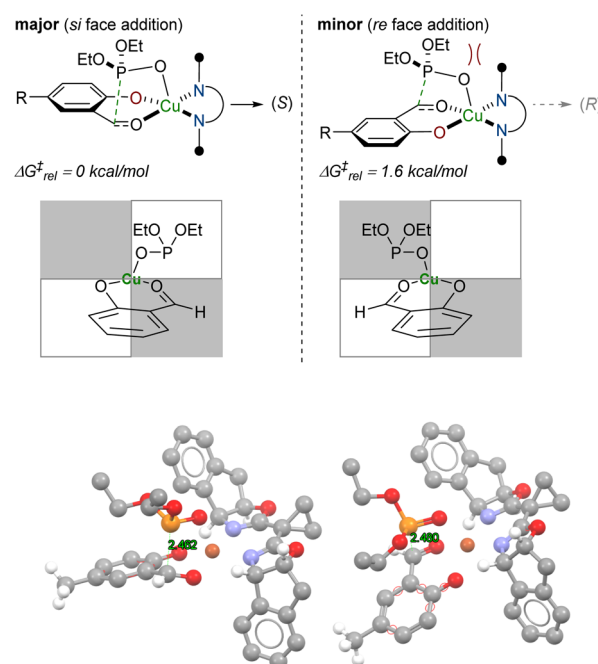

Fig. 2 Density functional theory-(DFT) calculated transition states for enantioselectivity-determining step of the of Pudovik reaction.

reside in apical sites. Admixture of this complex with diethyl phosphite led to the Pudovik adduct **2.11**. The direct outer sphere addition of phosphite to (indabox)Cu(**1.11**)$_2$ was deemed unlikely: the *re*-face of the aldehydes is more exposed for nucleophilic attack in this complex, which would lead to the minor (*R*)-product.
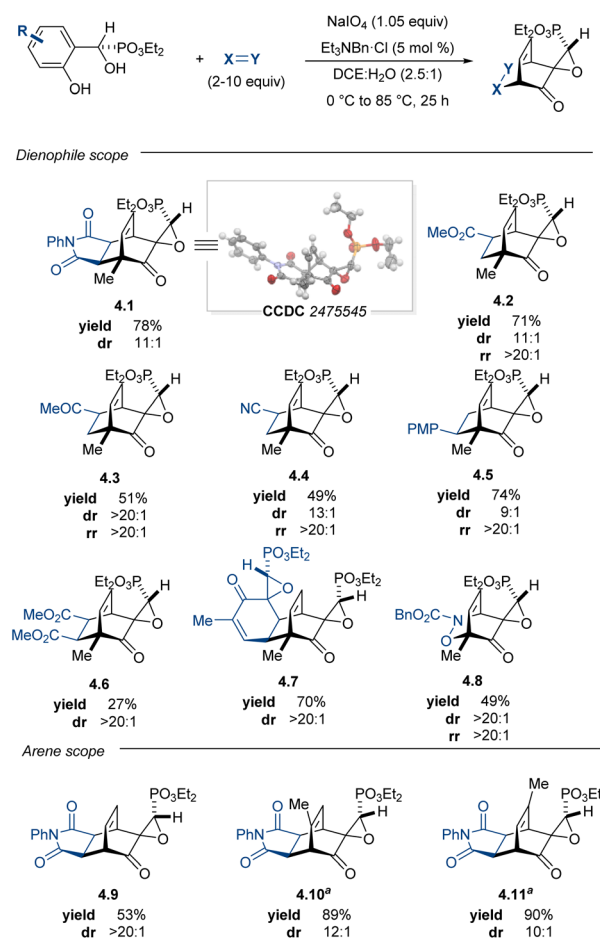
Carbonyl additions *via* the ternary complexes were evaluated using density functional theory at the level of M062X approximate functional and a compound Pople basis set in chloroform solvent (Fig. 2, see the SI for additional details). Visual inspection suggested differences in steric crowding for phosphite approach in the cyclic diastereomeric transition states, and the impact of these interactions was reflected in the lower calculated barrier for addition to the *si*-face ($\Delta\Delta G^{\ddagger} = 1.6$ kcal mol^{-1}). The analysis is predicated on a pre-equilibrium isomerization away from the more stable geometric isomer into one that is more reactive, intersecting with a more typical model of in-plane coordination of chelating substrates for Cu(II).[68] The absolute barrier for the P–C bond forming step is quite low (8.6 kcal mol^{-1}) despite the fact that nucleophilic addition to an anionic (X-type) ligand is obligatory.

To examine if the product could be acting as an additional stereodifferentiating ligand, we simulated the reaction at 50% conversion in the presence of freshly prepared catalyst (at the same concentration as our optimal conditions) using enantio-enriched **2.1**. The reaction proceeds to completion with no effect on stereoselectivity, indicating that the presence of enantioenriched product does not influence the stereoselectivity-determining step. The *ortho*-phenol proved critical for the title reaction to proceed: poor yield and enantioselectivity was observed with 2-methoxybenzaldehyde and 0% yield with *p*-vanillin (**2.14** and **2.15**). These observations further underscore the importance of covalent substrate activation.

Relaying chirality through a tandem dearomatization/cycloaddition sequence

With a developed method to access enantioenriched phenolic α-hydroxyphosphonates, we began investigating the behavior of these products in oxidative dearomatizations. Adaptation of Adler–Becker reactions conditions from a previous report from our lab[36] enabled a one-pot oxidative dearomatization/acylnitroso Diels–Alder cycloaddition; however, competitive oxidation of the α-hydroxyphosphonate to the putative corresponding acylphosphonate could not be suppressed. With this initial success, we examined the scope of suitable dienophiles and arenes that could be tolerated in this one-pot transformation. Pudovik adduct **2.2** performed well under optimized reaction conditions, furnishing maleimide adduct **4.1** in 78% yield and 11 : 1 dr (Table 3). As anticipated by our hypothesis, the stereochemical information imparted by the asymmetric Pudovik reaction was extended in the Adler–Becker oxidation to the adjacent spirocyclic center and the ensuing cycloaddition occurred diastereoselectively. The relative stereochemistry of the cycloaddition was confirmed by X-ray crystallographic analysis of cycloadduct **4.1**, with the Adler–Becker oxidation

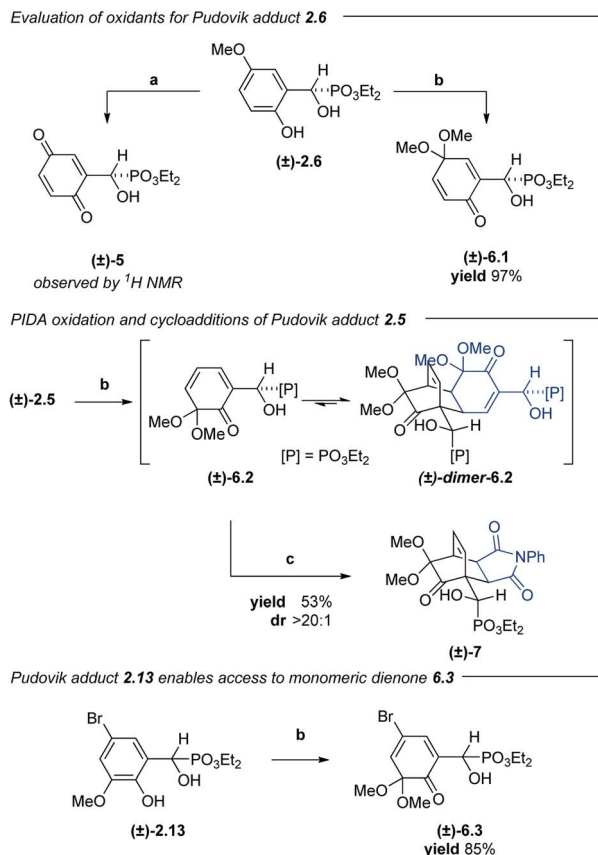**Table 3** Scope of one-pot Adler oxidation/[4 + 2]-cycloaddition

^{a} The reaction was performed at 0.03 M.

occurring stereoselectively and the subsequent cycloaddition occurring exclusively *syn* to the epoxide oxygen.[69]

Efforts to expand the scope to higher LUMO dienophiles were initially met with a few challenges. In addition to competing with oxidation to the achiral acyl phosphonate, dienone dimerization was competitive with the desired [4 + 2]-cycloaddition. Under standard reaction conditions, dimer **4.7** was isolated in 70% yield in a double diastereoselective cycloaddition. We hypothesized that this dimerization may be reversible at higher temperatures while the desired cycloaddition may provide a thermodynamic sink to sequester the target cycloadducts.[70] Indeed, subjecting the spiroepoxydienone dimer to 10 equiv. of dienophile at 85 °C produced the desired Diels–Alder adducts with excellent conversion and high regio- and diastereoselectivities. Oxidation occurred in under 3 h at 0–23 °C, at which point a dienophile could be added and the temperature raised to 85 °C to promote monomerization and the desired [4 + 2]-cycloaddition. Under these modified conditions, both normal and inverse-electron demand Diels–Alder cycloadducts were accessed in good yields and selectivities. Performing the reaction between 0 and 23 °C enabled access to

Evaluation of oxidants for Pudovik adduct 2.6

PIDA oxidation and cycloadditions of Pudovik adduct 2.5

Pudovik adduct 2.13 enables access to monomeric dienone 6.3

Scheme 2 Exploration of PIDA as alternative phenol oxidant. (a) NaIO$_4$, DCE : H$_2$O (2.5 : 1), TEBACl, 0 to 23 °C, 3 h. (b) PIDA, MeOH, 0 to 23 °C, 20 min. (c) *N*-Phenylmaleimide, CH$_2$Cl$_2$, 150 °C, 3 h.
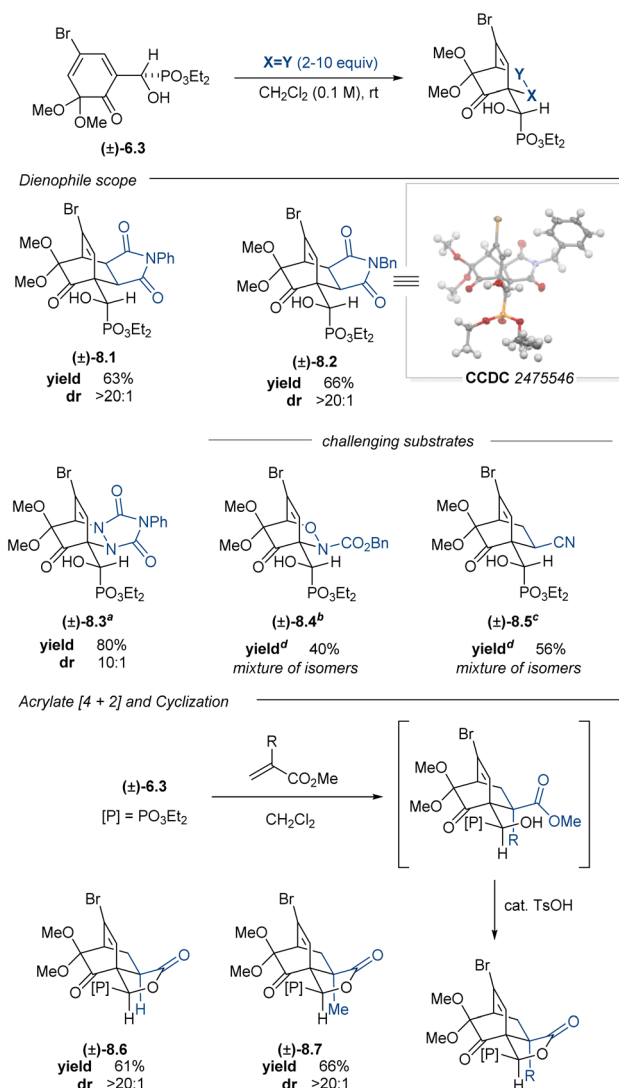
acylnitroso Diels–Alder adduct **4.8** in 49% yield as a single diastereomer and regioisomer. Maximum efficiency in the nitroso Diels–Alder reaction was achieved by dropwise addition of a hydroxycarbamate solution to a chilled mixture of starting material with excess sodium periodate, establishing an excess of diene relative to the active nitroso species, which has a very short lifetime.[36,71,72] While alkyl-substituted arenes were well-suited in this platform, unproductive reactivity was observed when using either of the methoxy-substituted Pudovik adducts (**2.5** and **2.6**), presumably due to formation of the corresponding quinone species (*e.g.* quinone (±)-**5**, Scheme 2). Brominated arenes **2.9** and **2.11** also underwent oxidation and cycloaddition; however, bromide displacement during oxidation led to complex reaction mixtures and incomplete conversion. Despite these substrate constraints, this method addresses the major limitations of our initial report,[36] providing comparable products in enantioenriched fashion and demonstrating an expansive scope of suitable dienophiles for this dearomative manifold.

In complementary investigations, α-hydroxyphosphonate (±)-**2.1** underwent dearomative oxidation by PIDA in methanol to give 2,5-cyclohexadienone (±)-**6.1** in 71% yield (not shown). Under similar conditions, α-hydroxyphosphonate **2.6** could also be dearomatized to give dienone (±)-**6.1** in 97% yield. Suspecting that the regioselectivity of this oxidation might be

heavily influenced by arene substitution patterns,[35] we subjected α-hydroxyphosphonate (±)-**2.5** to the same conditions to afford dimerized (±)-**6.2**. We anticipated that dienone (±)-**6.2** might behave similarly to the spiroepoxydienones with respect to cycloaddition reactivity. Indeed, heating of dimeric (±)-**6.2** at 150 °C in the presence of *N*-phenylmaleimide provided the desired cycloadduct (±)-**7** in 53% yield as a single diastereomer after purification. While this experiment demonstrated the propensity of these substrates to undergo both a reversible dimerization and a diastereoselective [4 + 2]-cycloaddition, we desired a platform that would enable cycloadditions to proceed under milder conditions.

2-Methoxy-4-substituted phenols oxidize to the corresponding 2,4-cyclohexadienones and dimerize much more slowly than

Table 4 Scope of [4 + 2]-cycloaddition with racemic dienone (±)-**6.3**

[a] 2 equiv. X=Y. [b] CbzNHOH (1.1 equiv.), CuCl$_2$ (0.1 equiv.), 2-ethyl-2-oxazoline (0.2 equiv.), air, 23 °C, 21 h. [c] 40 °C, 28 h. [d] Yields determined by ^{1}H NMR spectroscopic analysis using mesitylene as an internal standard.

the corresponding 4-unsubstituted phenols.[73] Aryl α-hydroxyphosphonate (±)-**2.13** was subjected to PIDA oxidation conditions to afford *ortho*-quinone monoketal (±)-**6.3** in 85% yield. Dimerization of this compound was slow in the solution phase and could be mitigated by immediate isolation to give monoketal (±)-**6.3** as a crystalline solid. Subsequent [4 + 2]-cycloadditions with normal-electron demand dienophiles proceeded well, furnishing cycloadducts (±)-**8.1**–**8.3** in good yields and good to excellent diastereoselectivities (Table 4). Given the promising preliminary data using α-hydroxyphosphonate (±)-**6.3** with the maleimide and PTAD dienophiles, we screened a nitroso carbamate dienophile and acrylonitrile ((±)-**8.4** and (±)-**8.5**); however, these cycloadditions proved to be poorly diastereoselective and regioselective, giving complex mixtures that could not be purified further. Cycloadditions with methyl acrylate and methyl methacrylate proceeded smoothly, affording a mixture of the predicted cycloadduct and the corresponding lactonized products (±)-**8.6** and (±)-**8.7**. The addition of catalytic quantities of *p*-toluenesulfonic acid (TsOH) to the reaction mixture converted the intermediate hydroxy esters to the lactones, which were isolated in 61% and 66% yields, respectively.

In contrast to quinone monoketal (±)-**6.3**, the enantioenriched dienone (*S*)-**6.3** did not readily crystallize, even upon purification. The corresponding oil dimerized upon standing at room temperature; however, this challenge was addressed by

Table 5 Scope of one-pot [4 + 2]-cycloaddition with enantioenriched Pudovik adduct **2.13**

devising a one-pot oxidative dearomatization/[4 + 2]-cycloaddition sequence. This strategy enabled the synthesis of enantioenriched cycloadducts in good yields and moderate to excellent diastereoselectivities (Table 5). This one-pot process enabled access to enantioenriched cycloadducts **8.1**–**8.3**, all with comparable yields to those reactions performed in two steps with the racemic material. The acrylate cycloadditions also proceeded smoothly in one-pot fashion, providing lactones **8.6** and **8.7** as single diastereomers in synthetically useful yields upon subjecting the crude reaction to catalytic quantities of TsOH. The enantioenrichment of the cycloadduct **8.7** matched that of the starting material, confirming that no racemization occurred during the oxidation or cycloaddition. This PIDA oxidation/[4 + 2]-cycloaddition sequence offers a complementary strategy to access cycloadducts bearing enantiomeric carbocyclic cores relative to the products from the Adler–Becker chemistry.
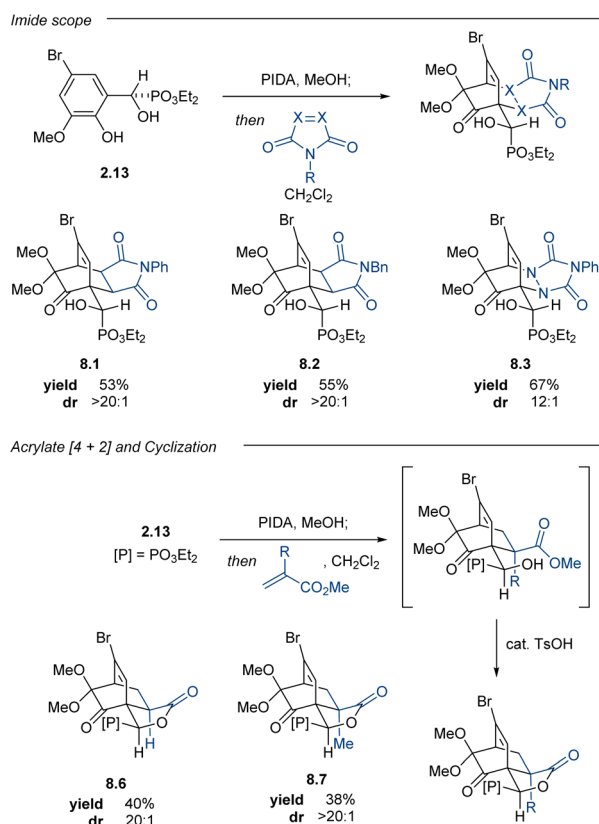
Complementary oxidation pathways reveal distinct mechanisms of stereoinduction

The influence of the stereogenic center established during the enantioselective phosphite/salicylaldehyde addition manifests itself in different ways depending on the chosen oxidant. For the Adler–Becker oxidation, the stereochemical outcome can be understood in stages (Fig. 3a). First, the cyclic I(VII) intermediate **II-NaIO₄** can lead to diastereomeric products depending on the illustrated gray or blue 90° bond rotation between the arene-benzylic C–C bond during the oxidative cyclization that extrudes the reduced I(V) fragment. The stereochemical relay to the *ipso*-carbon is highly selective, possibly due to a preference for the *trans*-phosphono epoxy ketone in the favored path.[74,75] In the second stage, the diastereotopic faces of **III** are sterically differentiated in a manner that precludes reagent approach *syn* to the phosphonate, thereby completing the stereochemical relay from the *ipso*-carbon to the asymmetric centers established in the cycloaddition.

The diastereofacial preference exhibited by hydroxyphosphonate dienones was ascertained by X-ray crystallographic analysis of cycloadduct (±)-**8.2**. Computational investigation suggested that hydrogen bonding between the α-hydroxyphosphonate and the incoming dienophile dictated the facial selectivity of the cycloaddition (Fig. 3b, directed model). Substrate pre-organization through internal chelation (Fig. 3b, internal chelate model) does not figure prominently as a stereocontrol feature ($\Delta\Delta G^{\ddagger} = 0.5$–$3.0$ kcal mol^{-1}, see Table S4 for more details). Exocyclic hydroxyl-directed cycloadditions have been reported;[76,77] however, this mode of selectivity generally requires a metal chelating agent to strengthen the interaction between the exocyclic alkoxy group and the incoming dienophile to achieve high selectivity.[78–80] A previous study from our own laboratories also suggests the hydrogen bonding through an exocyclic hydroxyl group can influence diastereoselectivity; however, the exact consequences of additional substitution appear system-dependent.[37]

The hydrogen-bonding hypothesis is further corroborated in this work by the decreased selectivity observed with acrylonitrile
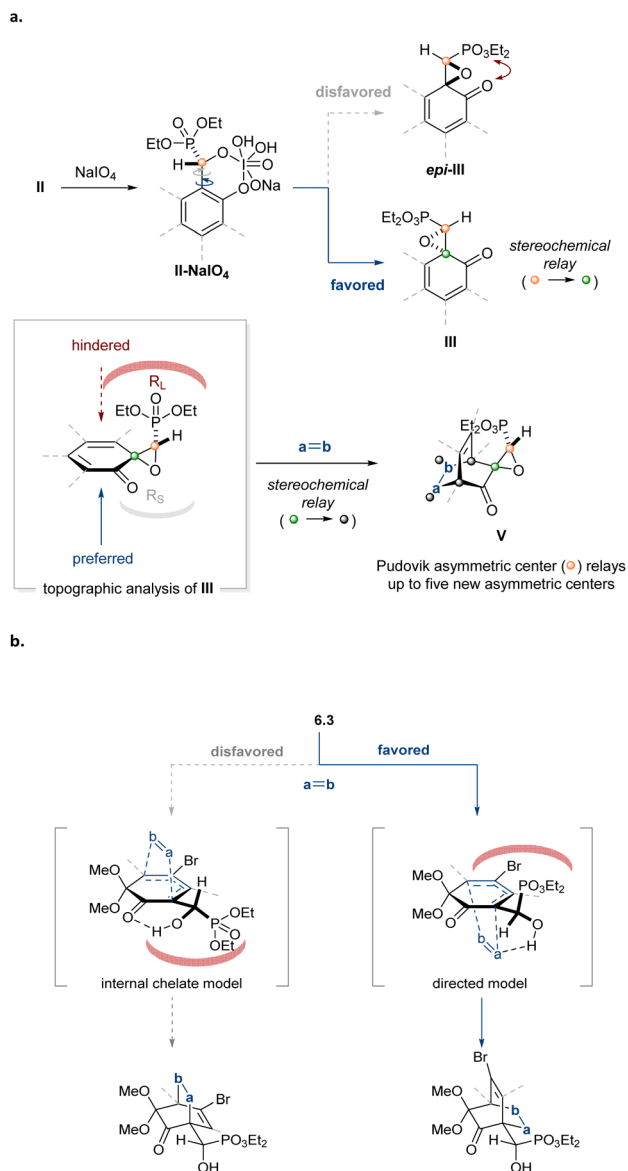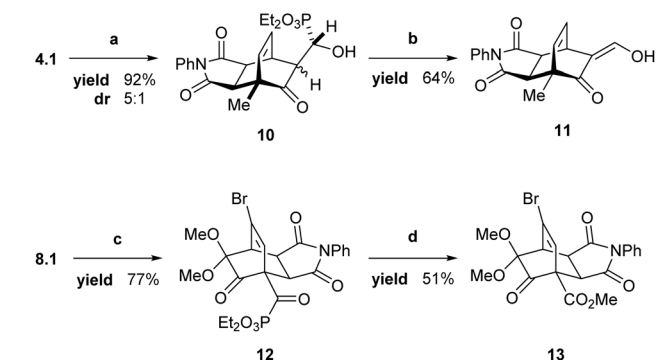
a.

b.

Fig. 3 (a) Steric constraints imposed by the rigid dialkoxyphosphinyl epoxide govern the facial selectivity of the cycloaddition. (b) Hydrogen-bonding between the α-hydroxyphosphonate and the dienophile directs facial selectivity of the cycloaddition.

adduct (±)-**8.5**, since this dienophile is unlikely to participate in the same degree of hydrogen bonding in the cycloaddition transition state as those dienophiles in the maleimide and acrylate cycloadditions. We hypothesize that the α-hydroxyphosphonate acts as a strong directing group due to enhanced acidity and hydrogen bond donor capability of the hydroxyl proton relative to that of an aliphatic or benzylic alcohol.

Leveraging the α-hydroxyphosphonate as a functional handle

To demonstrate the practicality of the described enantioselective dearomatization strategy, we desired a method that would leverage the α-hydroxyphosphonate as a diversifiable functional group. There exist several literature precedents for both the reductive epoxide opening and phosphonate expulsion

Scheme 3 Phosphite removal through reductive and oxidative paths. (a) Zn/AcOH, MeOH; (b) LiHMDS, TMSCl; then TFA, EtOH; (c) DMP, CH$_2$Cl$_2$; (d) Cu(OTf)$_2$, MeOH.

tranformations;[31,81] however, single-electron reductants including Cp$_2$TiCl and SmI$_2$ proved inadequate for promoting keto epoxide opening.[82] Instead, Zn/AcOH proved effective in opening epoxide **4.1** to the corresponding α-hydroxyphosphonate **10** in excellent yield and modest diastereoselectivity.[83] While the diastereomers were separable by chromatography, the selectivity proved inconsequential for phosphite removal in the subsequent step. The reported alkaline retro-Pudovik conditions[21,31] resulted in elimination of water and formation of a vinyl phosphonate species. To circumvent this competitive elimination, we developed an alternative procedure wherein deprotonation of intermediate **10** with excess LiHMDS and trapping of the α-alkoxyphosphonate with 1.2 equivalents of TMSCl provided the corresponding β-keto aldehyde **11** in 64% yield (Scheme 3), which existed predominantly as the enol tautomer. In contrast, the more sterically congested cycloadduct **8.1** could be oxidized to the corresponding acyl phosphonate **12**, which proved unexpectedly recalcitrant to nucleophilic acyl substitution.[28] To address that challenge, we developed a Cu(II)-catalyzed esterification that proceeded to afford methyl ester **13** in 51% yield.

Conclusions

In summary, we have developed a platform for the enantioselective dearomative functionalization of salicylaldehydes using an integrated asymmetric catalysis/oxidative dearomatization sequence. Stereodefined salicyl α-hydroxyphosphonates were synthesized using a new catalytic asymmetric Pudovik reaction. We anticipate that the reported Cu(II)-catalyzed transformation will inform further development of new enantioselective nucleophilic additions to salicylaldehydes. In the latter half of the described strategy, oxidative dearomatization enabled diversification of the phenolic cores to access distinct classes of enantioenriched cycloadducts with excellent diastereo- and regiocontrol. Lastly, we demonstrated the removal of the phosphonate functionality to access densely functionalized and stereochemically complex polycyclic scaffolds with ample functionality for applications towards complex molecule synthesis.

Author contributions

AJC and KAA: conceptualization; formal analysis; methodology; investigation; project administration; writing – original draft and editing. BKW: conceptualization; formal analysis; methodology; investigation; writing – original draft and editing. JGR: conceptualization; formal analysis; methodology. SL: investigation; formal analysis. JSJ: conceptualization; funding acquisition; supervision; project administration; writing – review and editing.

Conflicts of interest

There are no conflicts to declare.

Data availability

The data supporting this article have been included as part of the supplementary information (SI). Supplementary information: experimental procedures, characterization data, X-ray diffraction data, computational details of DFT studies. See DOI: https://doi.org/10.1039/d5sc08571c.

CCDC 2475547 ((indabox)Cu(**1.11**)$_2$), 2475545 (**4.1**) and 2475546 ((±)-**8.2**) contain the supplementary crystallographic data for this paper.[84a–c]

Acknowledgements

References

1 S. P. Roche and J. A. Porco, *Angew. Chem., Int. Ed.*, 2011, **50**, 4068–4093.

2 A. A. Rosatella and C. A. M. Afonso, *Biomedical and Biopharmaceutical Research*, 2024, **21**, 1–11.

3 J. L. Franklin, *J. Am. Chem. Soc.*, 1950, **72**, 4278–4280.

4 Y. You, S.-L. Yu, Q. Li, Y.-P. Zhang, Z.-H. Wang, J.-Q. Zhao, L. Yang and W.-C. Yuan, *ACS Catal.*, 2025, 9503–9543.

5 T. Dohi, A. Maruyama, N. Takenaga, K. Senami, Y. Minamitsuji, H. Fujioka, S. B. Caemmerer and Y. Kita, *Angew. Chem., Int. Ed.*, 2008, **47**, 3787–3790.

6 M. Uyanik, T. Yasui and K. Ishihara, *Angew. Chem., Int. Ed.*, 2010, **49**, 2175–2177.

7 M. Uyanik, T. Yasui and K. Ishihara, *Angew. Chem., Int. Ed.*, 2013, **52**, 9215–9218.

8 W. Sun, G. Li, H. Liang and R. Wang, *Org. Biomol. Chem.*, 2016, **14**, 2164.

9 S. A. Baker Dockrey, A. L. Lukowski, M. R. Becker and A. R. H. Narayan, *Nat. Chem.*, 2017, **10**, 119–125.

10 J. Zhu, N. P. Grigoriadis, J. P. Lee and J. A. Porco, *J. Am. Chem. Soc.*, 2005, **127**, 9342–9343.

11 S. Dong, J. Zhu and J. A. Porco, *J. Am. Chem. Soc.*, 2008, **130**, 2738–2739.

12 M. F. McLaughlin, E. Massolo, S. Liu and J. S. Johnson, *J. Am. Chem. Soc.*, 2019, **141**, 2645–2651.

13 R. J. Phipps and F. D. Toste, *J. Am. Chem. Soc.*, 2013, **135**, 1268–1271.

14 H. Egami, T. Rouno, T. Niwa, K. Masuda, K. Yamashita and Y. Hamashima, *Angew. Chem., Int. Ed.*, 2020, **59**, 14101–14105.

15 T. Stünkel, K. Siebold, D. Okumatsu, K. Murata, L. Ruyet, C. G. Daniliuc and R. Gilmour, *Chem. Sci.*, 2023, **14**, 13574–13580.

16 S. Chakrabarty, E. O. Romero, J. B. Pyser, J. A. Yazarians and A. R. H. Narayan, *Acc. Chem. Res.*, 2021, **54**, 1374–1384.

17 T. Hata, A. Hashizume, M. Nakajima and M. Sekine, *Tetrahedron Lett.*, 1978, **19**, 363–366.

18 R. E. Koenigkramer and H. Zimmer, *Tetrahedron Lett.*, 1980, **21**, 1017–1020.

19 E. Öhler, E. Zbiral and M. El-Badawi, *Tetrahedron Lett.*, 1983, **24**, 5599–5602.

20 J. Binder and E. Zbiral, *Tetrahedron Lett.*, 1984, **25**, 4213–4216.

21 G. Agnel and E. Negishi, *J. Am. Chem. Soc.*, 1991, **113**, 7424–7426.

22 J. Stawinski and A. Kraszewski, *Acc. Chem. Res.*, 2002, **35**, 952–960.

23 M. D. Khidre, *Phosphorus, Sulfur Silicon Relat. Elem.*, 2003, **178**, 2147–2158.

24 X. Linghu, J. R. Potnick and J. S. Johnson, *J. Am. Chem. Soc.*, 2004, **126**, 3070–3071.

25 R. Gancarz, I. Gancarz and U. Walkowiak, *Phosphorus, Sulfur Silicon Relat. Elem.*, 1995, **104**, 45–52.

26 A. Kraszewski and J. Stawinski, *Pure Appl. Chem.*, 2007, **79**, 2217–2227.

27 T. Cytlak, M. Skibińska, P. Kaczmarek, M. Kaźmierczak, M. Rapp, M. Kubicki and H. Koroniak, *RSC Adv.*, 2018, **8**, 11957–11974.

28 S. Chakrabarty and J. M. Takacs, *ACS Catal.*, 2018, **8**, 10530–10536.

29 R. Engel, in *Organic Reactions*, 2004, pp. 175–248.

30 F. A. Kortmann, M.-C. Chang, E. Otten, E. P. A. Couzijn, M. Lutz and A. J. Minnaard, *Chem. Sci.*, 2014, **5**, 1322–1327.

31 B. J. Rowe and C. D. Spilling, *J. Org. Chem.*, 2003, **68**, 9502–9505.

32 R. M. Moriarty, C. J. Chany II, J. W. Kosmeder II and J. D. Bois, in *Encyclopedia of Reagents for Organic Synthesis*, 2006.

33 R. Varala, V. Seema and N. Dubasi, *Organics*, 2023, **4**, 1–40.

34 A. A. Rosatella and C. A. M. Afonso, *ACS Omega*, 2022, **7**, 11570–11577.

35 D. Magdziak, S. J. Meek and T. R. R. Pettus, *Chem. Rev.*, 2004, **104**, 1383–1430.

36 S. N. Good, R. J. Sharpe and J. S. Johnson, *J. Am. Chem. Soc.*, 2017, **139**, 12422–12425.

37 J. G. Robins and J. S. Johnson, *Org. Lett.*, 2022, **24**, 559–563.

38 S. Quideau, L. Pouységu and D. Deffieux, *Synlett*, 2008, **2008**, 467–495.

39 L. Pouységu, D. Deffieux and S. Quideau, *Tetrahedron*, 2010, **66**, 2235–2261.

40 S. A. Beers, E. A. Malloy, W. Wu, M. P. Wachter, U. Gunnia, D. Cavender, C. Harris, J. Davis, R. Brosius, J. L. Pellegrino-Gensey and J. Siekierka, *Bioorg. Med. Chem.*, 1997, **5**, 2203–2211.

41 R. M. N. Kalla, H. R. Lee, J. Cao, J. W. Yoo and I. Kim, *New J. Chem.*, 2015, **39**, 3916–3922.

42 P. Merino, E. Marqués-López and R. P. Herrera, *Adv. Synth. Catal.*, 2008, **350**, 1195–1208.

43 J. P. Abell and H. Yamamoto, *J. Am. Chem. Soc.*, 2008, **130**, 10521–10523.

44 X. Zhou, X. Liu, X. Yang, D. Shang, J. Xin and X. Feng, *Angew. Chem., Int. Ed.*, 2008, **47**, 392–394.

45 D. Uraguchi, T. Ito and T. Ooi, *J. Am. Chem. Soc.*, 2009, **131**, 3836–3837.

46 K. Suyama, Y. Sakai, K. Matsumoto, B. Saito and T. Katsuki, *Angew. Chem., Int. Ed.*, 2010, **49**, 797–799.

47 D. Zhao and R. Wang, *Chem. Soc. Rev.*, 2012, **41**, 2095–2108.

48 T. Deng and C. Cai, *RSC Adv.*, 2014, **4**, 27853–27856.

49 J. Guin, Q. Wang, M. Van Gemmeren and B. List, *Angew. Chem., Int. Ed.*, 2015, **54**, 355–358.

50 B. R. Matthews, W. R. Jackson, G. S. Jayatilake, C. Wilshire and H. A. Jacobs, *Aust. J. Chem.*, 1988, **41**, 1697–1709.

51 P. J. Gerrits, J. Marcus, L. Birikaki and A. van der Gen, *Tetrahedron:Asymmetry*, 2001, **12**, 971–974.

52 H. Bühler, F. Effenberger, S. Förster, J. Roos and H. Wajant, *ChemBioChem*, 2003, **4**, 211–216.

53 J. D. White and S. Shaw, *Org. Lett.*, 2012, **14**, 6270–6273.

54 A. Zhang, L. Yang, N. Yang and Y. Liu, *Tetrahedron:Asymmetry*, 2014, **25**, 289–297.

55 S. V. Kumbhar and C. Chen, *Catal. Commun.*, 2021, **148**, 106166.

56 M. A. Tius and N. K. Reddy, *Synth. Commun.*, 1994, **24**, 859–869.

57 D. S. Yamashita, V. P. Rocco and S. J. Danishefsky, *Tetrahedron Lett.*, 1991, **32**, 6667–6670.

58 H. Kageji, N. Mori, H. Takikawa and H. Watanabe, *Tetrahedron*, 2018, **74**, 7074–7081.

59 E. Adler, K. Holmberg, H. Miyake, O. F. Nielsen, P. Klæboe and S. Kachi, *Acta Chem. Scand.*, 1971, **25**, 2775–2776.

60 E. Adler, S. Brasen, H. Miyake, O. F. Nielsen, P. Klæboe and S. Kachi, *Acta Chem. Scand.*, 1971, **25**, 2055–2069.

61 E. Adler, K. Holmberg, H. Kjøsen, S. Liaaen-Jensen, C. R. Enzell and B. Mannervik, *Acta Chem. Scand., Ser. B*, 1974, **28**, 465–472.

62 D. Gabrilidis, C. Kalogiros and L. Hadjiarapoglou, *Synlett*, 2004, **2004**, 2566–2569.

63 D. A. Evans, D. Seidel, M. Rueping, H. W. Lam, J. T. Shaw and C. W. Downey, *J. Am. Chem. Soc.*, 2003, **125**, 12692–12693.

64 J. N. Li, L. Liu, Y. Fu and Q. X. Guo, *Tetrahedron*, 2006, **62**, 4453–4462.

65 A. M. Liquori, A. Dami-ani, J. L. DeCoen, J. Mol Biol, D. Ajo, M. Bossa, A. Damiani, R. Fidenzi, S. Gigli, L. Lanzi, A. Lapiccirella, J. Theor Biol, W. S. Matthews, J. E. Bares, J. E. Bartmess, F. G. Bordwell, F. J. Cornforth, G. E. Drucker, Z. Margolin, R. J. McCallum, G. J. McCollum and N. R. Vanier, *J. Am. Chem. Soc.*, 2002, **97**, 7006–7014.

66 S. K. Ginotra and V. K. Singh, *Org. Biomol. Chem.*, 2007, **5**, 3932–3937.

67 B. J. Hathaway and D. E. Billing, *Coord. Chem. Rev.*, 1970, **5**, 143–207.

68 J. S. Johnson and D. A. Evans, *Acc. Chem. Res.*, 2000, **33**, 325–335.

69 V. Singh, *Acc. Chem. Res.*, 1999, **32**, 324–333.

70 R. Hashimoto, K. Hanaya, T. Sugai and S. Higashibayashi, *Bull. Chem. Soc. Jpn.*, 2022, **95**, 663–672.

71 G. W. Kirby, *Chem. Soc. Rev.*, 1977, **6**, 1–24.

72 A. D. Cohen, B.-B. Zeng, S. B. King and J. P. Toscano, *J. Am. Chem. Soc.*, 2003, **125**, 1444–1445.

73 C.-H. Lai, Y.-L. Shen, M.-N. Wang, N. S. Kameswara Rao and C.-C. Liao, *J. Org. Chem.*, 2002, **67**, 6493–6502.

74 E. Öhler, M. El-Badawi and E. Zbiral, *Chem. Ber.*, 1985, **118**, 4099–4130.

75 A. S. Demir, M. Emrullahoglu, E. Pirkin and N. Akca, *J. Org. Chem.*, 2008, **73**, 8992–8997.

76 K. N. Houk, S. R. Moses, Y. D. Wu, N. G. Rondan, V. Jager, R. Schohe and F. R. Fronczek, *J. Am. Chem. Soc.*, 1984, **106**, 3880–3882.

77 H.-C. Tseng, A. K. Gupta, B.-C. Hong and J.-H. Liao, *Tetrahedron*, 2006, **62**, 1425–1432.

78 D. E. Ward and M. S. Abaee, *Org. Lett.*, 2000, **2**, 3937–3940.

79 L. Barriault, P. J. A. Ang and R. M. A. Lavigne, *Org. Lett.*, 2004, **6**, 1317–1319.

80 L. W. K. Moodie and D. S. Larsen, *Eur. J. Org Chem.*, 2014, **2014**, 1684–1694.

81 G. Agnel and E. Negishi, *J. Am. Chem. Soc.*, 1991, **113**, 7424–7426.

82 D. B. G. Williams, J. Caddy and K. Blann, *Org. Prep. Proced. Int.*, 2003, **35**, 307–360.

83 V. K. Singh, P. T. Deota and A. V. Bedekar, *J. Chem. Soc., Perkin Trans. 1*, 1992, 903–912.

84 (*a*) CCDC 2475545: Experimental Crystal Structure Determination, 2025, DOI: 10.5517/ccdc.csd.cc2p3094; (*b*) CCDC 2475546: Experimental Crystal Structure Determination, 2025, DOI: 10.5517/ccdc.csd.cc2p30b5; (*c*) CCDC 2475547: Experimental Crystal Structure Determination, 2025, DOI: 10.5517/ccdc.csd.cc2p30c6.